J Mater Sci (2010) 45:4689–4695
DOI 10.1007/s10853-010-4305-y

ULTRAFINE GRAINED MATERIALS

Microstructure evolution through heavy compression aided by thermodynamic calculations

Farideh Hajiakbari · Mahmoud Nili-Ahmadabadi · Behrang Poorganji · Tadashi Furuhara

Received: 17 December 2009 / Accepted: 6 February 2010 / Published online: 20 February 2010

Abstract The induced martensite transformation in a dual-phase bainitic ferrite–austenite steel during heavy compression was studied by thermodynamic computations. Compression tests were conducted at temperatures of 298 and 573 K on the rectangle samples at the strain rate of 0.001 s^{-1}. The samples were deformed to 40 and 70% of their original thickness. It was found that 70% compression of the steel at room temperature resulted in transformation of retained austenite to martensite, which is in agreement with thermodynamic calculations. Additionally, heavy compression resulted in the formation of fine grains with high angle grain boundaries which confirms grain refinement.

Introduction

Grain refinement of different metallic alloys has recently been regarded as a method to improve simultaneously strength and toughness. One of the most effective techniques which can be appropriated to produce ultrafine-grained (UFG) materials is severe plastic deformation [1–4]. Nowadays, this method has successfully been used to produce several UFG steels, such as low-carbon steel [5, 6], ferrite–martensite dual-phase steel [7], and age hardenable steel [1]. One of the drawbacks in making UFG high Si bainitic steel is the presence of retained austenite. Retained austenite through severe plastic deformation may transform to martensite [8] and cause ductility reduction. Therefore, developing a model which could predict induced martensite transformation at temperatures higher than martensite start temperature (M_s) is very useful. The influence of external stress, on M_s, has been discussed qualitatively [9]. In this matter, Patel and Cohen [10] developed a model for calculating the effect of uniaxial tension and compressive stresses on the M_s of iron–nickel and iron–nickel–carbon steels. Also, based on thermodynamic calculations, Xie et al. [11] studied the strain-induced martensite formation in a manganese steel medium through impact loading condition. In this paper, it is attempted to develop a thermodynamic model which predicts induced martensite transformation based on the driving force of austenite to martensite transformation ($\Delta G^{\gamma \rightarrow M}$) and mechanical energy (U) during compression process. In the latter, the microstructure evolutions of the steel through compression process are studied at different temperatures and the calculations are verified by experimental results.

Experimental

In order to study a dual-phase bainitic ferrite–carbon enrichment austenite steel, a high Si bainitic steel (Fe–0.22C–2.0Si–3.0Mn) was selected. Four rectangular billets (8.5 mm × 8.5 mm × 12 mm dimensions) were austenited at 900 °C. Reducing the austenite grain size, austenitization was performed at various stages which differ in duration; followed by austempering at 330 °C for 30 min [12]. Then, specimens were deformed at 298 and 573 K to 40 and 70% of their original thickness (Table 1). Compression process was performed at the strain rate of 0.001 s^{-1}.

F. Hajiakbari · M. Nili-Ahmadabadi (✉)
School of Metallurgy and Materials Engineering, University of Tehran, P.O. Box 11155-4563, Tehran, Iran
e-mail: nili@ut.ac.ir; nili@chamran.ut.ac.ir

B. Poorganji · T. Furuhara
Institute for Materials Research, Tohoku University, 2-1-1 Katahira, Aoba-ku, Sendai, Japan

Table 1 Specimens dimension before and after deformation procedure

Test temperature (K)	573	298
Deformation percent (%)	70	40
Initial height (mm)	12	12
Final height (mm)	3.3	7.1

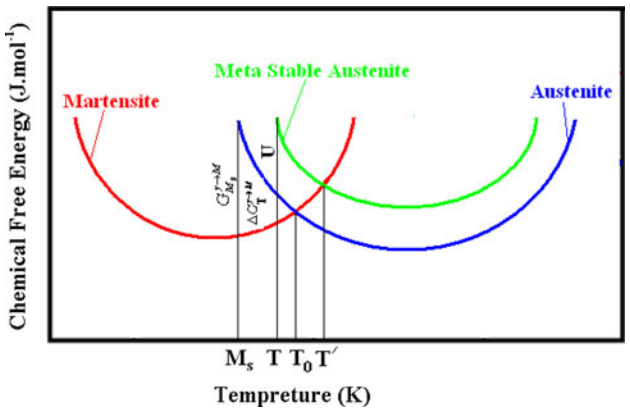

Fig. 1 Free energy change versus temperature [13]

The microstructure of the as-received and 70% deformed samples were examined using scanning electron microscopy (SEM). Also, the microstructure of samples after 70% compression possess were studied by electron back scattering diffraction (EBSD) technique, with a step size of 0.2 μm. To examine the microstructures precisely, X-ray diffraction (XRD) analysis was conducted on the deformed samples with angular range 70–85° 2θ with Cu Kα radiation at 40 kV and 30 mA in a step scanning at 0.05° 2θ with a count time of 30 s per point. In the case of as-received sample, X-ray diffraction was conducted by using Co Kα radiation, with angular range 45–125°.

Thermodynamic calculation

In this study, the thermodynamic model which was developed for austenite to martensite transformation during ECAP process [13] is adapted for simple pressure process.

It is well established that at temperatures higher than M_s, austenite does not transform to martensite in the absence of an external stress. In other words, induced martensite can appear when the required driving force is supplied by mechanical energy. It is derived from Fig. 1 that the mechanical energy can supply enough driving force for martensitic transformation at temperatures higher than M_s and below M_d, due to enhancement of free energy of austenite phase (metastable austenite curve). Therefore, the driving force for martensitic transformation at test temperature consists of chemical driving force $\left(\Delta G_T^{\gamma\rightarrow M}\right)$ and mechanical energy (U).

Mechanical energy calculation

The area under stress–strain curve is the mechanical energy per unite volume which is consumed by the material during deformation. A reliable approach to determine this area is multiplying the max value of the applied stress by its corresponding strain. So, the mechanical energy (U) could be defined by two terms; shear energy $(\tau\bar{\gamma})$ which is shear stress in the direction of habit plane multiplication at the effective shear strain and normal energy $(\sigma\bar{\varepsilon})$ is the normal stress, perpendicular to the habit plane, multiplication at effective normal strain. Thus, [10]:

$$U = \tau\bar{\gamma} + \sigma\bar{\varepsilon} \tag{1}$$

τ is positive, as most of the habit planes shear in one direction. However, normal stress in some situations induces martensite formation and prevents martensite formation in other situations. For tensile stress, σ is positive while negative for the pressing stress. In order to compute the mechanical energy, the parameters mentioned are determined as follows.

Effective strain

It is known that the effective strain is represented by [14]:

$$\bar{\varepsilon} = \frac{\sqrt{2}}{3}\left[(\varepsilon_z - \varepsilon_y)^2 + (\varepsilon_y - \varepsilon_x)^2 + (\varepsilon_x - \varepsilon_z)^2\right]^{1/2} \tag{2}$$

where ε_x, ε_y, and ε_z are the plastic strains in the directions of x, y, and z, respectively. The normal strain in the direction of applied compression (ε_z) is as follows [14]:

$$\varepsilon_z = \mathrm{Ln}\left(\frac{h_1}{h_2}\right) \tag{3}$$

where h_1 and h_2 are the initial and final height of the sample (Table 1), respectively.

Also, it is well established that during the plastic region, the material flows with negligible change in the volume. Assuming constant volume, the following equation is derived [14]:

$$\varepsilon_x + \varepsilon_y + \varepsilon_z = 0 \tag{4}$$

On the other hand, in an isotropic material, the strains in the x and y directions (ε_x, ε_y) are equal [14]. Thus,

$$\varepsilon_x = \varepsilon_y \tag{5}$$

Considering Eqs. 4 and 5, ε_x and ε_y could be evaluated as a function of ε_z

Table 2 Calculated strain values

Parameter	$\varepsilon_{x_{40\%}}$, $\varepsilon_{y_{40\%}}$	$\varepsilon_{z_{40\%}}$	$\bar{\varepsilon}_{40\%}$	$\bar{\gamma}_{40\%}$	$\varepsilon_{x_{70\%}}$, $\varepsilon_{y_{70\%}}$	$\varepsilon_{z_{70\%}}$	$\bar{\varepsilon}_{70\%}$	$\bar{\gamma}_{70\%}$
Magnitude	−0.26	0.52	0.52	0.74	−0.65	1.3	1.3	1.86

$$\varepsilon_x = \varepsilon_y = -\frac{\varepsilon_z}{2} \tag{6}$$

Substituting Eq. 3 into Eq. 6, the above equation can be written as:

$$\varepsilon_x = \varepsilon_y = -\frac{1}{2}\mathrm{Ln}\left(\frac{h_1}{h_2}\right) \tag{7}$$

Finally, substituting the normal strain components in Eq. 2, it is easy to calculate the effective normal strain. In addition, the effective shear strain could be determined as follows [14]:

$$\bar{\gamma} = \sqrt{2}\bar{\varepsilon} \tag{8}$$

The normal strain components in 40 and 70% deformed samples are calculated by using Eq. 7, which are shown in Table 2. In the next step, the effective normal strains (for the both samples) are determined by substituting the normal strain components in Eq. 2. Also, the effective shear strains are evaluated by applying Eq. 8.

Effective stress

For uniaxial tension or compression stresses, a consideration of Mohr's circle shows that the resolved shear and normal stresses are [10]

$$\begin{aligned} \tau &= 0.5\bar{\sigma}\sin 2\theta \\ \sigma &= 0.5\bar{\sigma}(1+\cos 2\theta) \end{aligned} \tag{9}$$

where $\bar{\sigma}$ is the effective plastic stresses (tension or compression) and θ is the angle between the specimen axis and the normal to any potential habit plane. The effective plastic stress is represented by [14]

$$\bar{\sigma} = \frac{\sqrt{2}}{2}\left[(\sigma_z-\sigma_y)^2+(\sigma_y-\sigma_x)^2+(\sigma_x-\sigma_z)^2\right]^{1/2} \tag{10}$$

where σ_x, σ_y, and σ_z are plastic stress in the directions of x, y, and z, respectively. Further, Holloman equation can be applied to calculate the plastic stress in the direction of applied pressure [14]

$$\sigma_z = k\varepsilon_z^n \tag{11}$$

where k and n are work-hardening factor and work-hardening exponent, respectively. Here, it is assumed that the effect of the temperature variations on the work-hardening factor and work-hardening exponent of the steel is negligible. In order to determine stresses in the direction of x and y, Levy–Mises equation could be applied [14]

$$\frac{\varepsilon_x}{\sigma_x} = \frac{\varepsilon_y}{\sigma_y} = \frac{\varepsilon_z}{\sigma_z} \tag{12}$$

Substituting the ε_x, ε_z, and σ_z in Eq. 12, the σ_x is calculated. In the same way, the σ_y is determined. Consequently, the effective stress could be evaluated from Eq. 10.

The normal stresses in the direction of applied pressure (in 40 and 70% deformed samples) are calculated by substituting n, k (0.58 and 1947 MPa, respectively [13]) and ε_z values in Eq. 11 (Table 3). Then, σ_x and σ_y for both deformed samples are determined from Eq. 12. Lastly, the effective normal stresses are computed by substituting normal stress components in Eq. 10 (Table 3).

Mechanical energy

Now, the mechanical energy (U) could be expressed as a function of the orientation of a transformation martensitic plate by substituting Eq. 9 into Eq. 1 [10]

$$U = 0.5\bar{\gamma}\cdot\bar{\sigma}\sin 2\theta \pm 0.5\bar{\varepsilon}\cdot\bar{\sigma}(1+\cos 2\theta) \tag{13}$$

The above equation could be used for calculating mechanical energy either in macroscopic or microscopic approach [10, 13]. Therefore, Eq. 13 in the microscopic scale could be written as

$$U = 0.5\gamma_0\cdot\bar{\sigma}\sin 2\theta \pm 0.5\varepsilon_0\cdot\bar{\sigma}(1+\cos 2\theta) \tag{14}$$

where γ_0 and ε_0 are shear and normal strains through martensitic transformation, which here assumed to be 0.25 and 0.03 [15], respectively. Since we are concerned with the plates that form first (at M_s) under the influence of applied stress, it is necessary to find the particular orientation which yields a maximum value of U [10]

$$\frac{\mathrm{d}U}{\mathrm{d}\theta} = \gamma_0\bar{\sigma}\cos 2\theta \pm \varepsilon_0\bar{\sigma}(-\sin 2\theta) = 0 \tag{15}$$

$$\frac{\sin 2\theta}{\cos 2\theta} = \tan 2\theta = \pm\frac{\gamma_0}{\varepsilon_0} \tag{16}$$

Substituting the known components of the transformation strain into Eq. 16, the 2θ value assumed to be 85°. On the

Table 3 Calculated stress values

Parameter	$\sigma_{x_{40\%}}$ and $\sigma_{y_{40\%}}$ (MPa)	$\sigma_{z_{40\%}}$ (MPa)	$\bar{\sigma}_{40\%}$ (MPa)	$\sigma_{x_{70\%}}$ and $\sigma_{y_{70\%}}$ (MPa)	$\sigma_{z_{70\%}}$ (MPa)	$\bar{\sigma}_{70\%}$ (MPa)
Magnitude	−670	1330	2000	−1130	2270	3400

other hand, it is known in the macroscopic scale austenite planes shear in direction of 45° which yields the 2θ value 90°. As the similar values are calculated in the both approaches, it seems logical to assume planes in the macroscopic and microscopic scale shear in the same direction. In this matter, 2θ value assumed to be 90°. Then, by substituting the values of 2θ, effective stress, effective normal, and shear strains in Eq. 13, the mechanical energy through simple compression could be calculated as follows

$$\begin{aligned} U_{70\%} &= 0.5 \times 1.86 \times 3400 \times \sin(90) - 0.5 \times 1.3 \times 3400 \\ &\quad \times (1 + \cos(90)) \\ &= 952 \text{ MPa} = 6570 \text{ J mol}^{-1} \end{aligned}$$

$$\begin{aligned} U_{40\%} &= 0.5 \times 0.74 \times 2000 \times \sin(90) - 0.5 \times 0.52 \times 2000 \\ &\quad \times (1 + \cos(90)) \\ &= 220 \text{ MPa} = 1520 \text{ J mol}^{-1} \end{aligned}$$

Chemical energy calculation

The martensite start temperature of the proposed steel (for infinity large austenite grain) was estimated 154 K [13]. However, considering the effect of austenite grain size reduction on the M_s, the M_s of the steel was calculated by using Bhadeshia equation [16] equals to 67 K [13]. Also, the driving force of the austenite to martensite transformation could be calculated as follows [17]

$$\begin{aligned} \Delta G^{\gamma\to M} &= 2xRT\ln x + x(H_\alpha - \Delta H_\gamma - (\Delta S_\alpha - \Delta S_\gamma)T \\ &\quad + 4\omega_\alpha - 6\omega_\gamma) - 4RT(1-x)\ln(1-x) \\ &\quad + 5RT(1-2x)\ln(1-2x) - 6RTx\ln\left|\frac{\delta_\gamma - 1 + 3x}{\delta_\gamma + 1 - 3x}\right| \\ &\quad - 6RT(1-x)\ln\left|\frac{1 - 2J_\gamma + (4J_\gamma - 1)x - \delta_\gamma}{2J_\gamma(2x-1)}\right| \\ &\quad + 3RTx\ln(3-4x) + 4RTx\ln\left|\frac{\delta_\alpha - 3 + 5x}{\delta_\alpha + 3 - 5x}\right| \\ &\quad + (1-x)\Delta G_{\text{Fe}}^{\gamma\to\alpha} + \Delta f^* \end{aligned} \tag{17}$$

where R, T, and x are the gas constant, absolute temperature, and mole fraction of carbon, respectively. Other parameters are determined as follows [13, 18, 19]

$$\delta_\alpha = \left|9 - 6x(2J_\alpha + 3) + (9 + 16J_\alpha)x^2\right|^{1/2} \tag{18}$$

$$\delta_\gamma = \left|1 - 2x(1 + 2J_\gamma) + (1 + 8J_\gamma)x^2\right|^{1/2} \tag{19}$$

$$J_{\alpha,\gamma} = 1 - \exp(-\omega_{\alpha,\gamma}/RT) \tag{20}$$

$$\omega_\alpha = 48570 \text{ J mol}^{-1}$$

$$\omega_\gamma = 8523 \text{ J mol}^{-1}$$

$$\Delta H_\alpha = 112212 \text{ J mol}^{-1}$$

$$\Delta S_\alpha = 51.5 \text{ J mol}^{-1}$$

$$\Delta H_\gamma = 35129 + 169105x \tag{21}$$

$$\Delta S_\gamma = 7.639 + 120.4x \tag{22}$$

$$\Delta f^* = -1746 \text{ J mol}^{-1}$$

$$\begin{aligned} \frac{\Delta G_{\text{Fe}}^{\gamma\to\alpha}}{RT} &= 5\ln\left|\frac{1-x}{1-2x}\right| \\ &\quad + 6\ln\left|\frac{1 - 2J_\gamma + (4J_\gamma - 1)x - \left\{1 - 2(1 + 2J_\gamma)x + (1 + 8J_\gamma)x^2\right\}^{1/2}}{2J_\gamma(2x-1)}\right| \end{aligned} \tag{23}$$

Substituting the mole fraction of austenite carbon content of the proposed steel (0.05 [13]) in the above equations, all the parameters are known. As a result, $\Delta G^{\gamma\to M}$ at M_s, 573 and 298 K could be computed by using equation (17) as follows:

$$\Delta G_{M_s}^{\gamma\to M} = 7040 \text{ J mol}^{-1}$$

$$\Delta G_{298}^{\gamma\to M} = 645 \text{ J mol}^{-1}$$

$$\Delta G_{573}^{\gamma\to M} = -221 \text{ J mol}^{-1}$$

Consequently, the required mechanical energy for induced martensite formation at each temperature is:

$$\Delta G_{M_s}^{\gamma\to M} - \Delta G_{298}^{\gamma\to M} = 7040 - 645 = 6395 \text{ J mol}^{-1}$$

$$\Delta G_{M_s}^{\gamma\to M} - \Delta G_{573}^{\gamma\to M} = 7040 - (-221) = 7261 \text{ J mol}^{-1}$$

The above values confirm that the transformation of austenite to martensite is only feasible, if the energy difference between $\Delta G^{\gamma\to M}$ at M_s and test temperature is supplied by mechanical energy. The required mechanical energy for formation of martensite at 298 K is 6395 J mol^{-1}, whereas the mechanical energy through 70 and 40% compression are 6570 and 1520 J mol^{-1}, respectively. Thus, based on the thermodynamic calculations, it is expected that induced martensite appears only at heavy (70%) deformed steel at room temperature. On the other hand, the applied mechanical energy during 40 and 70% compression process is lower than the required mechanical energy for martensite formation at 573 K (7261 J mol^{-1}), which means that the formation of induced martensite is not possible. It should be noted that carbon distribution in the austenite phase is assumed to be uniform. However, the carbon may distribute heterogeneously, usually the austenite phase in the interlath has a higher carbon content than the other region which in turn the martensitic transformation appears firstly in the lower carbon enriches austenite [20].

Experimental results

Figure 2 illustrates the microstructure and the XRD diffraction of the as-received sample. It can be seen (Fig. 2a)

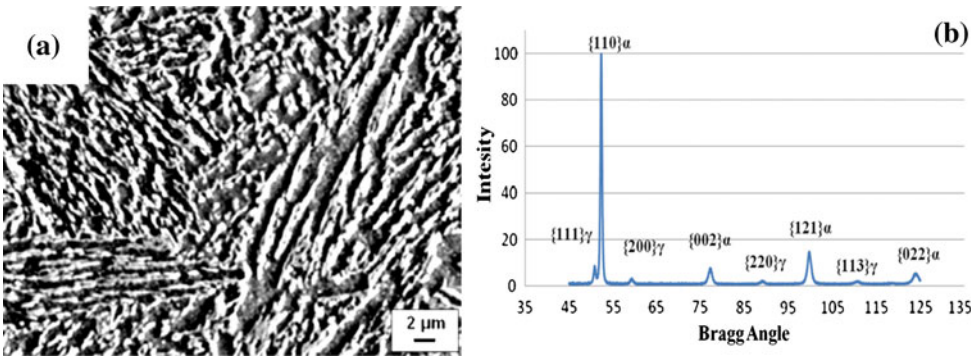

Fig. 2 **a** SEM micrograph and **b** XRD pattern of the as-received specimen

that the microstructure of the as-received sample consists of acicular bainitic ferrite and thin film retained austenite. It is known that the reduction of austempering temperature leads to enhancement of the carbon content of austenite. Thus, austempering at relative low temperature (330 °C) results in the formation of carbon-enriched austenite [21]. On the other hand, reduction of austempering temperature increases the driving force of bainitic transformation. So, austempering at lower temperature persuades formation of acicular bainitic ferrite and increases hardness of steel. Also, Fig. 2b shows that the initial sample consists of ferritic bainite and retained austenite in which their volumetric fractions are 83 and 17%, respectively.

SEM micrograph of samples after deformation at 298 and 573 K are presented in Fig. 3. It can be seen that the shear component of the applied stress resulted in formation oriented microstructures. As it is expected, the oriented structure enhanced by increasing the temperature, due to easier glide of dislocations at higher temperature. In order to study the microstructure evolution and determining the misorientation of grain boundary, the EBSD micrograph of the 70% deformed samples (at both temperatures) was used (Fig. 4). It can be seen that the heavy deformed steel at 573, the size of bainitic ferrite blocks reduces from about 50 μm to 500 nm. The mentioned phenomenon resulted from the formation of fine grains with high-angle grain boundaries (grain-refinement mechanism).

However, in some blocks partial of low-angle boundaries does not transform to high-angle boundaries and needs more mechanical energy for formation of fine grains. Also, the grain size decreases by increasing the test temperature. On the other hand, since dislocations sliding are easier at higher temperature and the active sliding systems increase by temperature at the bainitic ferrite structure, the micrographs of the deformed sample at 573 K are finer than similar sample at 298 K.

XRD pattern of the deformed samples is shown in Fig. 5. It is derived that the {220} pick of austenite had removed after 70% compression at room temperature. This phenomenon could be attributed to the transformation of retained austenite to martensite, during severe plastic deformation of the steel, which is in agreement with thermodynamic calculations. However, as the thermodynamic model predicts, the induced martensite does not form after 40% deformation at room temperature and the austenite pick is visible. Further, according to the thermodynamic model, the applied mechanical energy at 573 K (for both 40 and 70% deformed steels) is not enough for the austenite to martensite transformation and the austenite pick remains unchanged after deformation.

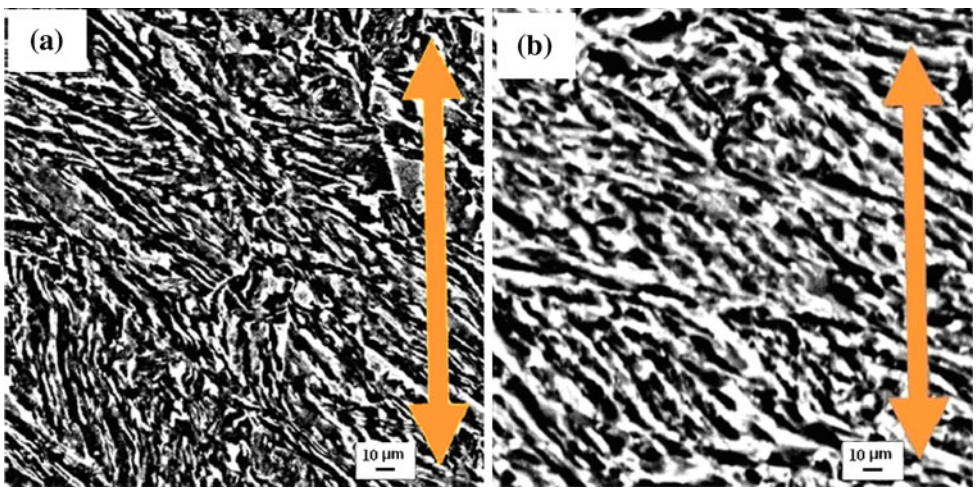

Fig. 3 SEM micrograph of 70% deformed samples at **a** 573 K and **b** 298 K

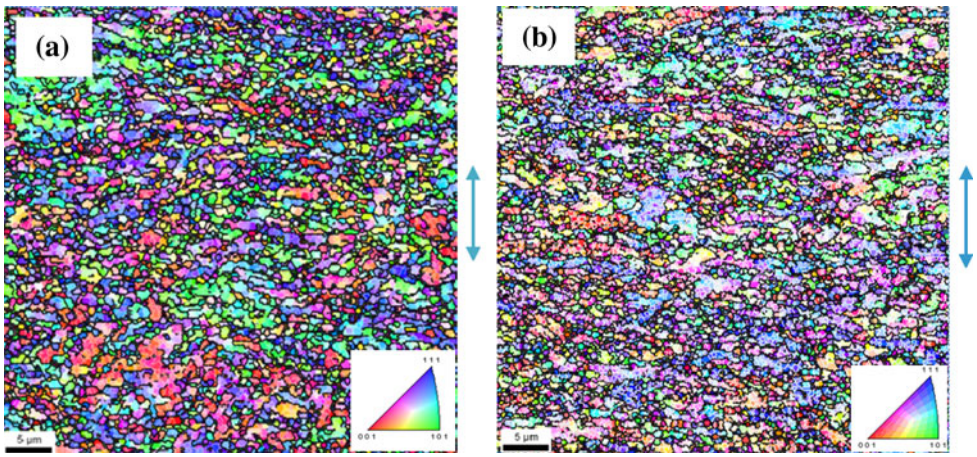

Fig. 4 EBSD micrograph of 70% deformed samples at **a** 573 K and **b** 298 K

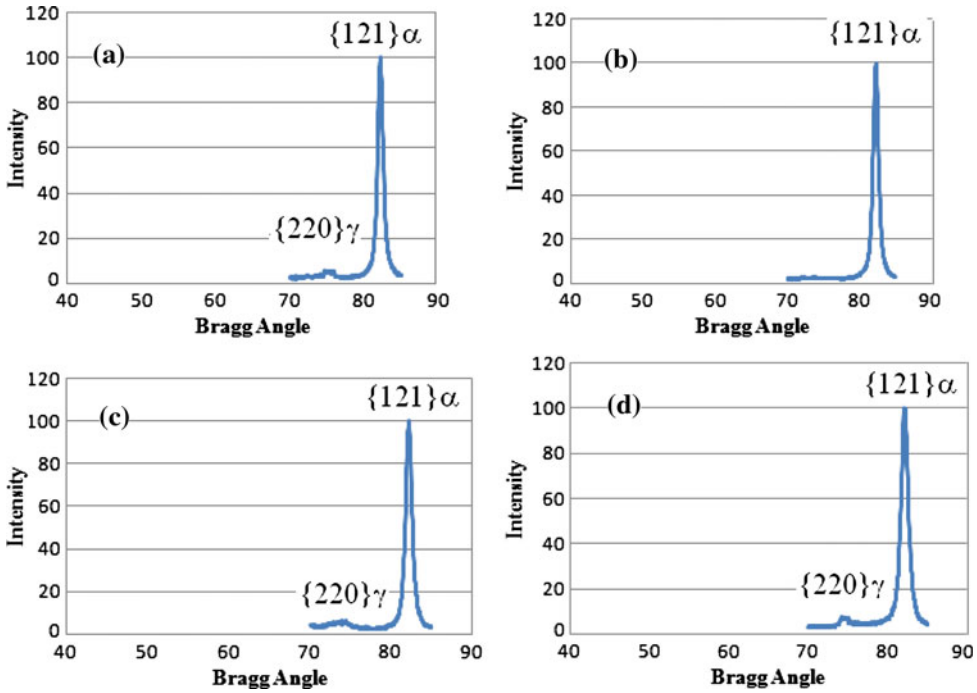

Fig. 5 XRD pattern of the deformed samples: **a** 40% and **b** 70% deformed at 298 K, **c** 40%, and **d** 70% deformed at 573 K

Summary and conclusions

In this paper, the effect of single pressure on the microstructural evolution of a high Si bainitic steel was studied. It was found that the applied mechanical energy through deformation (40 and 70%), at 573 K, is not enough for the austenite to martensite transformation. Thus, it is expected that austenite dose not transform to martensite during deformation at 573 K, which is in agreement with XRD pattern of the sample. However, as it is predicted by thermodynamic model, induced martensite appears during 70% deformation at room temperature and the XRD pattern of the sample shows the decrease in the austenite pick. On the other hand, 70% compression resulted in formation of fine grains with high-angle grain boundaries which conforms grain-refinement phenomena.

Acknowledgements The authors would like to express their thanks to the Iran National Science Foundation for financial support of this research and also thank Dr. Parsa for fruitful discussions.

References

1. Iranpour Mobarake M, Nili-Ahmadabadi M, Poorganji B, Fatehi A, Shirazi H, Furuhara T, Habibi Parsa M, Hossein Nedjad S (2008) Mater Sci Eng A 491(1–2):172
2. Iwahashi Y, Furukawa M, Horita Z, Nemoto M, Langdon TG (1998) Metall Mater Trans A 29(9):2245

3. Valiev RZ, Islamgaliev RK, Alexandrov IV (2000) Prog Mater Sci 45(1–4):103
4. Huang CX, Wang K, Wu SD, Zhang ZF, Li GY, Li SX (2006) Acta Mater 54(3):655
5. Shin DH, Kim YS, Lavernia EJ (2001) Acta Mater 49(13):2387
6. Fukuda Y, Oh-Ishi K, Horita Z, Langdon TG (2002) Acta Mater 50(6):1359
7. Son Y, Lee YK, Park KT, Lee CS, Shin DH (2005) Acta Mater 53(11):3125
8. Chatterjee S, Bhadeshia HKDH (2007) Mater Sci Technol 23:1101
9. Fisher JC, Turnbull D (1953) Acta Metall 1(3):310
10. Patel JR, Cohen M (1953) Acta Metall 1(5):531
11. Xie J, Zhu Y, Wang X (2000) J Mater Sci Technol 16:449
12. Nili-Ahmadabadi M, Hajiakbari F, Rad F, Karimi Z, Iranpour M, Poorganji B, Furuhara T (2010) J Nanosci Nanotechnol 10
13. Nili-Ahmadabadi M, Hajiakbari F, Poorganji B, Furuhara T (2010) Acta Mater
14. Dieter GE (1988) In: Rosa I (ed) Mechanical metallurgy. McGraw-Hill, New York, pp 43–72
15. Ivanisenko Yu, MacLaren I, Sauvage X, Valiev RZ, Fecht H-J (2006) Acta Mater 54(6):1659
16. Yang HS, Bhadeshia HKDH (2009) Scr Mater 60(7):493
17. Bell T, Owen WS (1967) Trans Met Soc AIME 239:1940
18. Bhadeshia HKDH, Edmonds DV (1980) Acta Metall 28(9):1265
19. Bhadeshia HKDH (1981) Met Sci 15:178
20. Nili Ahmadabadi M (1997) Metall Mater Trans A 28(10):2159
21. Porter DA, Easterling KE (1986) Diffusionless transformation. Phase transformations in metals and alloys. Van Nostrand Reinhold, Berkshire, p 388